PROCEEDINGS OF SCIENCE

# Thermal properties of neutron stars in the framework of density-dependent nuclear field theory

**Rodrigo Negreiros***
*Computational Science Research Center and Department of Physics, San Diego State University*
*E-mail:* negreiro@sciences.sdsu.edu

**Fridolin Weber**†
*Department of Physics, San Diego State University*
*E-mail:* fweber@sciences.sdsu.edu

We investigate the composition, structure and thermal evolution of neutron stars for nuclear equations of state that are computed in the framework of an effective density-dependent nuclear field theory. Special attention is paid to the hyperon populations of neutron star matter predicted by such a theory. The results are compared with the outcome obtained from standard (non-density dependent) nuclear field theory.

*10th Symposium on Nuclei in the Cosmos*
*July 27–August 1, 2008*
*Mackinac Island, Michigan, USA*

*Speaker.

†Supported by the National Science Foundation under Grant PHY-0457329, and by the Research Corporation.

 

PoS(NIC X)187

## 1. Relativistic nuclear field-theoretical models for the EoS

Many relativistic nuclear field-theoretical studies of neutron star matter are performed for the relativistic mean field (RMF), relativistic Hartree-Fock (RHF), and relativistic Brueckner-Hartree-Fock (RBHF) approximations [1]. This is different in this paper, which treats neutron star matter in the framework of a relativistic density-dependent (DD) nuclear field theory [2], based on the Lagrangian [2, 3]

$$\begin{aligned}\mathscr{L} = &\sum_B \bar{\psi}_B \left(i\gamma_\mu \partial^\mu - m_B\right)\psi_B + \frac{1}{2}\sum_{i=\sigma,\delta}\left(\partial_\mu \Phi_i \partial^\mu \Phi_i - m_i^2 \Phi_i^2\right) - \frac{1}{2}\sum_{\kappa=\omega,\rho}\left(\frac{1}{2}F^\kappa_{\mu\nu}F^{\kappa\mu\nu} - m_\kappa^2 A^\kappa_\mu A^{\kappa\mu}\right)\\ &+\bar{\psi}_B\hat{\Gamma}_\sigma(\bar{\psi}_B,\psi_B)\psi_B\Phi_\sigma - \bar{\psi}_B\hat{\Gamma}_\omega(\bar{\psi}_B,\psi_B)\gamma_\mu\psi A^{\omega\mu} + \bar{\psi}_B\hat{\Gamma}_\delta(\bar{\psi}_B,\psi_B)\tau\psi_B\Phi_\delta\\ &-\bar{\psi}_B\hat{\Gamma}_\rho(\bar{\psi}_B,\psi_B)\gamma_\mu\tau\psi_B A^{\rho\mu} + \sum_{l=e,\mu}\bar{\psi}_l\left(i\gamma_\mu\partial^\mu - m_l\right)\psi_l\,, \end{aligned} \tag{1.1}$$

with $F^\kappa_{\mu\nu} = \partial_\mu A^\kappa_\nu - \partial_\nu A^\kappa_\mu$. This Lagrangian describes baryons ($B = p, n, \Sigma, \Xi, \ldots$) interacting via the exchange of mesons ($\sigma, \omega, \rho, \delta$). In RMF, RHF and RBHF the meson-baryon vertices $\hat{\Gamma}_\alpha$ ($\alpha = \sigma, \omega, \delta, \rho$) are density-independent quantities given by expressions like $\hat{\Gamma}_\sigma = ig_\sigma$ in case of the scalar $\sigma$ meson, or by $\hat{\Gamma}^\mu_\omega = g_\omega\gamma^\mu + (i/2)(f_\omega/2m)\partial_\lambda[\gamma^\lambda,\gamma^\mu]$ in case of $\omega$ mesons [1]. This is different for the DD framework where the meson-baryon vertices $\hat{\Gamma}_\alpha$ depend on the baryon field operators $\psi_B$ [2]. We consider both types of vertices in this paper. Schematically, the nuclear field equations that follow from (1.1) have the mathematical form

$$(i\gamma^\mu\partial_\mu - m_B)\psi_B(x) = \sum_{M=i,\kappa} M(x)\,\hat{\Gamma}_M\,\psi_B(x)\,,\quad (\partial^\mu\partial_\mu + m_\sigma^2)\sigma(x) = \sum_B \bar{\psi}_B(x)\,\hat{\Gamma}_\sigma\,\psi_B(x)\,, \tag{1.2}$$

plus similar equations for the other mesons [1, 2]. Here, we consider solutions of the nuclear field equations that are computed for the relativistic mean-field (Hartree) approximation and the relativistic density-dependent method described in [2]. The solutions are referred to as HV [1] and

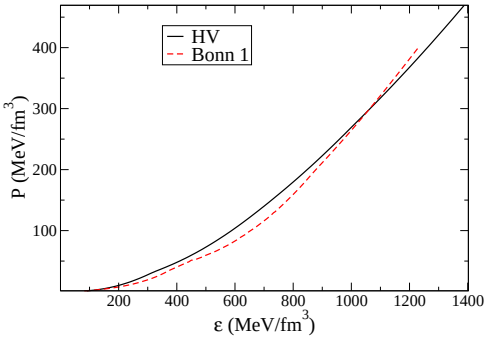


**Figure 1:** HV and Bonn EoS. The latter is computed for density dependent baryon-meson vertices.

Bonn [4], respectively. The parameters of the Lagrangian are adjusted to the bulk properties of nuclear matter, which are: saturation energy, $E/A = -16.0$ MeV, symmetry energy, $a_4 = -32.5$ MeV, compressibility modulus, $K = 200$ to 300 MeV, and

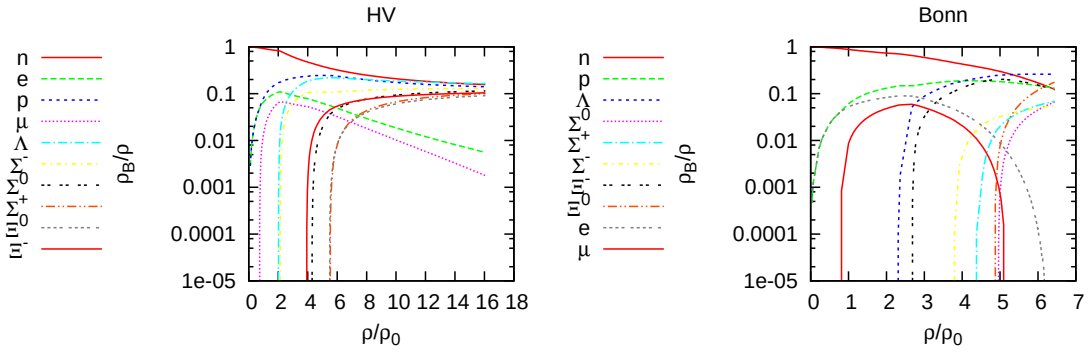


**Figure 2:** Sample neutron star matter compositions for HV and Bonn.

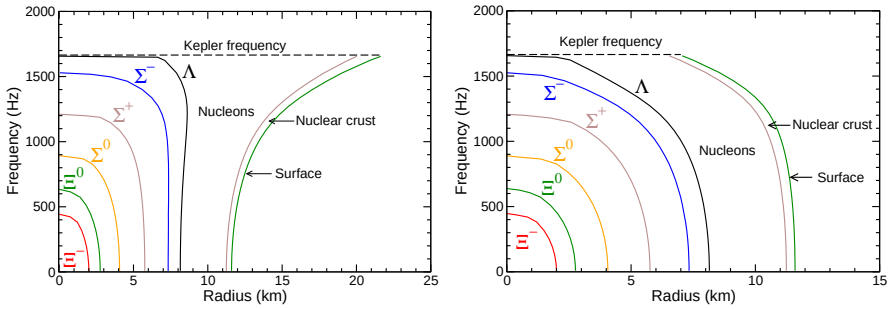


**Figure 3:** Hyperon composition for a rotating neutron star in equatorial (left) and polar (right panel) directions.

effective nucleon mass, $m^* = 0.74$ to $0.82$, at saturation density of $\rho_0 = 0.16$ fm$^{-3}$. The equations of state (EoS) computed from the field equations are plotted in Fig. 1, and the and the respective particle populations for non-rotating as well as rotating stars [1] are shown in Fig. 2 and 3. One sees that the EoS obtained for the DD model differs only very little from the standard EoS, HV. This is not so for the respective particle populations, which are very different. In this paper the variables $P$, $\varepsilon$ and $\rho$ represent pressure, energy density and number density respectively.

## 2. Stellar structure equations and thermal evolution

Solving Einstein's equation of a spherically symmetric star [1], leads to the Tolman–Oppenheimer–Volkoff equation, given by

$$\frac{dP}{dr} = -\frac{\varepsilon\, m}{r^2}\frac{(1+P/\varepsilon)\left(1+4\pi r^3 P/m\right)}{1-2m/r}\,, \tag{2.1}$$

which describes the properties of neutron stars. We use units for which the gravitational constant and velocity of light are $G = c = 1$ so that the mass of the sun is $M_\odot = 1.47$ km. The mass contained in a sphere of radius $r$ is given by $m = 4\pi\int_0^r r^2\varepsilon dr$. Hence the total gravitational mass of a neutron star follows as $M \equiv m(R)$, where $R$ denotes the star's radius. The masses of neutron stars lie between about one and two solar masses, and their radii are around 10 km to 15 km. Thus,

one estimates that $2M/R \sim 30-60\%$ for neutron stars. Solutions of the TOV equation computed for HV and Bonn are shown in Fig. 4. The horizontal line at $M = 1.0 \pm 0.2 M_{\odot}$ refers to X-ray

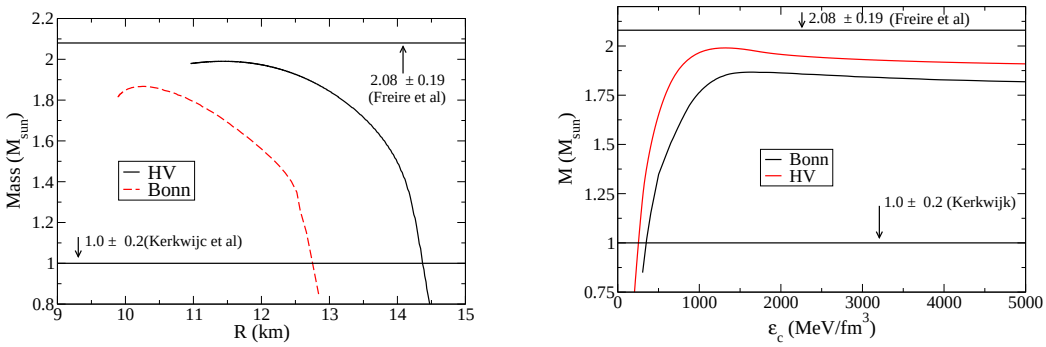


**Figure 4:** Mass-radius relationship (left panel) and neutron star mass versus central density (right panel) for the EoS of this paper. The horizontal lines represent minimum and maximum observed neutron star masses.

binary 4U1538-52 [5] , while the upper limit $2.08 \pm 0.19 M_{\odot}$ denotes the mass of the potentially very heavy neutron star in the globular cluster M5 [6]. The density-dependent model studied here does not support a neutron star that massive.

The predominant cooling mechanism of hot, newly formed neutron stars immediately after formation is neutrino emission, with an initial cooling time scale of seconds. Already a few minutes after birth, the internal neutron star temperature drops to around $\sim 10^9$ K. Photon emission overtakes neutrino emission when the internal temperature has fallen to $\sim 10^8$ K, with a corresponding surface temperature roughly two orders of magnitude smaller. Neutrino cooling dominates for at least the first $10^3$ years, and typically for much longer in standard cooling (modified Urca) calculations. The dominant neutrino emitting processes in neutron star matter are summarized in [1, 7]. In this work superfluidity is not considered. The general relativistic equations that govern the thermal evolution of neutron stars are [1]

$$\frac{\partial L_r}{\partial M} = -\frac{Q_\nu}{\rho\sqrt{1-\frac{2M}{r}}} - \frac{C_\nu}{\rho\sqrt{1-\frac{2M}{r}}}\frac{\partial T}{\partial t}, \quad \frac{\partial \ln T}{\partial M} = \nabla \frac{\partial \ln P}{\partial M}, \tag{2.2}$$

where $T$ is the stellar temperature, $C_\nu$ is the specific heat at a constant volume, and $Q_\nu$ is the neutrino emissivity [8]. Figure 5 shows solutions of these equations for the two EoS studied in this paper. The calculations are performed for neutron star masses of $1.4 M_{\odot}$ and $1.8 M_{\odot}$, in order to illustrate the influence of different neutron star compositions on the cooling history of neutron stars. As can be seen from Fig. 5, standard neutron star cooling leads to good agreement with observed cooling data for both stellar masses, while enhanced cooling via the direct URCA process (among neutrons, protons, and hyperons) reduces the stellar temperature way too quickly, leading to temperatures that are not in agreement with observed data. Another important feature of these calculations is that we use consistent values for the effective masses of baryons, computed self-consistently from the field equations (1.2), rather than a fixed value (usually $\sim 0.7 m_n$) throughout

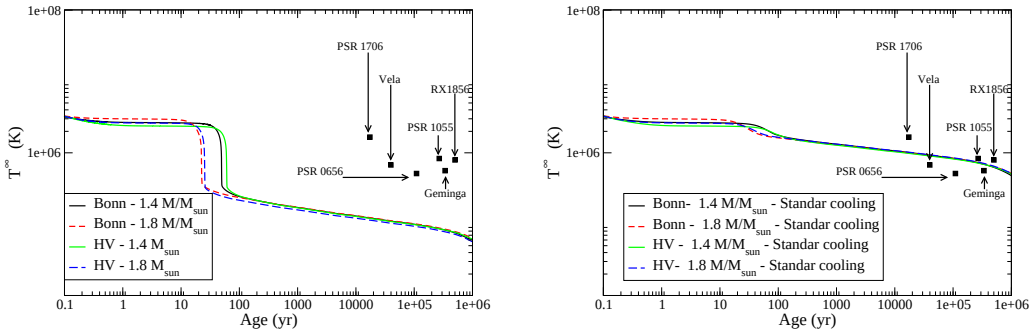


**Figure 5:** Cooling behavior of 1.4 and 1.8 $M_{\odot}$ neutron stars (left panel: enhanced cooling via direct URCA; right panel: standard cooling). Observed data are from [9].

the star, which has important consequences for stellar cooling. Like the effective nucleon mass, the specific heat and the thermal conductivity of the stellar matter were consistently computed from the underlying population of baryons and leptons as well.

The next step in our research will bear on the exploration of the cooling behavior of rotating neutron stars. In contrast to non-rotating neutron stars, whose particle compositions do not change with time (that is, they are frozen in), rotating neutron stars can experience drastic density changes during spin-down as isolated radio pulsars or during spin-up as X-ray accreters in LMXBs. Either way, any such changes in rotational frequency are inevitably accompanied by the re-arrangement of matter in the ultra-dense stellar cores of neutron stars and may even lead to the creation respectively destruction of novel states of ultra-dense neutron star matter, like quark matter, or a condensate of $K^-$ bosons [1]. The thermal evolution of rotating neutron stars is therefore not determined by their initial core compositions at birth, but needs to be computed self-consistently with a numerical, general relativistic, rotation code coupled to a stellar cooling code.

## References

[1] F. Weber, *Pulsars as Astrophysical Laboratories for Nuclear and Particle Physics*, High Energy Physics, Cosmology and Gravitation Series (IOP Publishing, Bristol, Great Britain, 1999).

[2] F. Hofmann, C. M. Keil, and H. Lenske, Phys. Rev. C **64** (2001) 034314.

[3] F. Weber, R. Negreiros, P. Rosenfield, and M. Stejner, Prog. Part. Nucl. Phys. 59 (2007) 94.

[4] F. Weber, R. Negreiros, and P. Rosenfield, EJPA **33** (2007) 381.

[5] M.H. van Kerkwijk, J. van Paradijs and E.J. Zuiderwijk, Astron. Astrophys. **303**, 497 (1995).

[6] P. C. C. Freire, A. Wolszczan, M. van den Berg and J. W. T. Hessels. Astrophys. J. **679**, 1433 (2008).

[7] D. Page, U. Geppert, and F. Weber, Nucl. Phys. **A 777** (2006) 492.

[8] M. Prakash, M. Prakash, J. M. Lattimer, and C. J. Pethick, Astrophys. J. **390** (1992) L77.

[9] D. Page, J. M. Lattimer, M. Prakash, and A. W. Steiner, Astrophys. J. Suppl. **155** (2006) 497.